Engineering with Computers (2023) 39:1127–1141
https://doi.org/10.1007/s00366-021-01498-1

ORIGINAL ARTICLE

An efficient computational model for vibration behavior of a functionally graded sandwich plate in a hygrothermal environment with viscoelastic foundation effects

Mohamad W. Zaitoun[1] · Abdelbaki Chikh[3,4] · Abdelouahed Tounsi[1,2,3,5] · Alfarabi Sharif[1] · Mohammed A. Al-Osta[1,5] · Salah U. Al-Dulaijan[1,5] · Mesfer M. Al-Zahrani[1,5]

Received: 24 May 2021 / Accepted: 7 August 2021 / Published online: 1 September 2021

Abstract
This paper introduces the free vibrational response solution of a functionally graded (FG) "sandwich plate" resting on a viscoelastic foundation and subjected to a hygrothermal environment load using an accurate high-order shear deformation theory. In this study, three different types of FG "sandwich plate" geometries were investigated. Only four unknowns were considered in the displacement field, including an indeterminate integral, along with a sinusoidal shape function to represent transverse shear stresses. Hamilton's principle was utilized to obtain the equation of motion by considering infinitesimal deformation theory combined with a generalized Hook's law. The variables studied are the damping coefficient, aspect ratio, volume fraction density, moisture and temperature variation, and thickness. The results showed that the increase in damping coefficient (c_t) as a property of the viscoelastic foundation would enhance the free-vibrational response of the plate. However, the degree of enhancement would be influenced by the hygrothermal environment.

Keywords Vibration · Sandwich plate · Functionally graded material · Viscoelastic foundation · FGM · Hygrothermal · Non-uniform temperature

1 Introduction

Lightweight sandwich structures which adopt a high stiffness–weight ratio and a high strength–weight ratio have been manufactured and used for engineering applications such as in the aircraft industry [1–8]. However, classic sandwich plates are incapable of withstanding high-temperature environments. A new class of composite materials that has drawn extensive attention is functionally graded materials (FGMs) [1, 9]. A typical FGM is an inhomogeneous composite structure made up of different phases of material constituents (usually ceramic and metal) with a high bending–stretching coupling effect. By gradually varying the volume fraction of the constituent materials, their material properties show a smooth and continuous change from one surface to another, consequently eliminating interface problems and mitigating thermal stress concentrations [10–12]. By merging the extraordinary behavior of FGM in conjunction with the sandwich plate, researchers have tried to investigate the behavior of an FGM "sandwich plate" (FGSP). Moreover, as the FGSP uses three layers, this opens the door to studying the plate with a range of different possibilities. Considering FG face sheets and a homogeneous core is one case that is investigated from different perspectives [13–23]. On the other hand, FGM could be placed in the core of an FGSP, and the other two faces could be comprised of either FGM or homogeneous sheets [13, 16, 24–28]

Nguyen [29] proposed a "high-order shear deformation theory" (HSDT) to evaluate the dynamic behavior of an

✉ Abdelouahed Tounsi
tou_abdel@yahoo.com

1 Department of Civil and Environmental Engineering, King Fahd University of Petroleum and Minerals, Dhahran 31261, Eastern Province, Saudi Arabia

2 YFL (Yonsei Frontier Lab), Yonsei University, Seoul, Korea

3 Material and Hydrology Laboratory, Faculty of Technology, Civil Engineering Department, University of Sidi Bel Abbes, Sidi Bel Abbès, Algeria

4 Université Ibn Khaldoun, BP 78 Zaaroura, 14000 Tiaret, Algeria

5 Interdisciplinary Research Center for Construction and Building Materials, KFUPM, Dhahran, Saudi Arabia

FG sandwich beam; moreover, HSDT is used frequently to solve composite problems as it reaches the solution accurately and efficiently compared to others [30]. An analytical solution was developed using a method employing Lagrange multipliers for three different boundary conditions (simply supported–simply supported, clamped–clamped, and clamped–free). Zenkour investigated the effect of trigonometric shear deformation theory on a "sandwich plate" behavior with FG faces in terms of buckling and natural frequency [31]. Meksi et al. [32] proposed an HSDT and impeded an indeterminate integral term in the displacement field to evaluate the bending, buckling, and vibrational behavior of an FGSP with a homogeneous core and FG face sheets. Di Sciuva [33] investigated the vibration and buckling behavior of an FG carbon nanotube reinforced sandwich plate using an extended refined Zigzag theory in parallel with the Ritz method. The mechanical behavior of FGSP resting on an elastic foundation and subjected to a thermal environment while using refined quasi-3D shear deformation theory was studied by Mahmoudi et al. [34]. Ghumare et al. [35] considered a new fifth-order shear deformation theory accounting for transverse shear and normal deformations to analyze the bending behavior of an FG plate subjected to a hygro-thermal environment and resting on an elastic foundation. Fu [27] utilized a two-dimensional differential quadrature (DQ) method developed by Bellman [36] in the calculation of an nth order shear deformation theory to evaluate the free vibrational response of an FGSP resting on an elastic foundation. Madenci [37] extended the method of Mixed Finite Element Method (MFEM) to account for static and vibrational analysis, while other works continued evolving numerical techniques to optimize the solution using methods such as Artificial Neural Networks (ANN) [38–40]. Nebab et al. [36] considered a nonlinear elastic foundation in deriving the dynamic behavior of FG plates using the four-unknown shear deformation theory. Akbas et al. [37] investigated the case of an FG thick beam resting on a viscoelastic foundation focusing on the dynamic responses under a dynamic sine pulse load. The case of FG nanobeams resting on a viscoelastic foundation was further investigated by Ebrahimi et al. [41]. They studied the effect of a hygrothermal environment on the dynamic behavior of FG nanobeams using nonlocal strain gradient theory.

The increase of temperature and moisture concentration exposure on the structures has a very strong adverse impact on its performance. Therefore, the dynamic properties of an FGSP resting on a viscoelastic foundation will be affected when subjected to this type of exposure. In addition, the literature review showed that no research work is conducted on the vibrational behavior of the FGSP resting on a viscoelastic foundation and subjected to a hygrothermal environment. Therefore, the impact of the damping coefficient for the viscoelastic foundation of the plate using an efficient "four-unknown" HSDT with sine function is explored, along with the effect induced by hygro-thermal conditions on the FGSP. FGSP will be modeled as a continuous variation of material constituents along the thickness using a "power law variation." Therefore, the material properties would change gradually. The analytical solutions for the "fundamental frequency" of an FGSP resting on a viscoelastic foundation can be obtained using Navier's procedure.

1.1 Sandwich assembly

This study considers a rectangular FGSP. Cartesian coordinate (x, y, z) systems are utilized to describe the infinitesimal deformations of a typical plate. The origin of a "sandwich plate" with respect to z $(z = 0)$ is considered to be at the middle surface of the plane. The top and bottom surfaces are defined at $= \pm h/2$. The material properties vary along the z-direction continuously based on the following power law equation:

$$P((n))(z) = P_{\mathrm{m}} + \left(P_{\mathrm{c}} - P_{\mathrm{m}}\right)V_n, \tag{1}$$

where n denotes the number of each layer $n = (1,2,3)$, while $P_{\mathrm{c}} and P_{\mathrm{m}}$ denote the properties of ceramic and metal of the FGSP, respectively. The volume fraction $\left(V_n\right)$ of the material is defined below for each FGSP. The effective change of the material properties in the direction of Z, such as Young's modulus (E), thermal expansion coefficient (α), moisture expansion coefficient (β) and mass density (ρ) are considered in Eq. (1). We consider in this work three types of FG Sandwich Plate as shown in Figs. 1, 2 and 3.

1.2 Types of FG sandwich plate

Type A: sandwich plate with homogeneous ceramic core and FG face sheets.

This type of sandwich plate has a ceramic core, and the top and bottom layers are FGM sheets. The top layer is metallic on its upper surface and ceramic on the lower side. In contrast, the bottom layer is metallic on its lower surface and ceramic on its upper surface. The volume fraction $\left(V_n\right)$ of the ceramic in this type can be determined by the following formulas [42]:

$$\begin{aligned} V_1 &= \left(\frac{1 + 2\overline{z}}{1 + 2H1}\right)^r, \quad -\frac{1}{2} \le \overline{z} \le H_1, \\ V_2 &= 1, \quad H_1 \le \overline{z} \le H_2, \\ V_3 &= \left(\frac{1 - 2\overline{z}}{1 - 2H2}\right)^r, \quad H_2 \le \overline{z} \le 1/2 \end{aligned} \tag{2}$$

where $\overline{z} = z/h$ and $H_j = h_j/h\,(j = 1,2)$. $(r \ge 0)$ represents the material index. A fully homogeneous ceramic plate is in the case of $r = 0$. However, it is a metal–ceramic–metal plate (m–c–m) when $r \to \infty$.

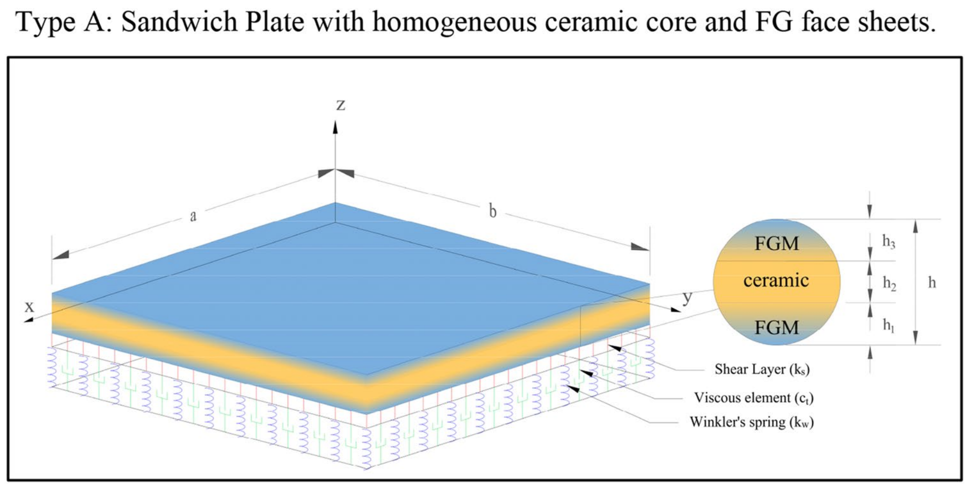

Fig. 1 Illustration of FGSP resting on the viscoelastic foundation: Type A

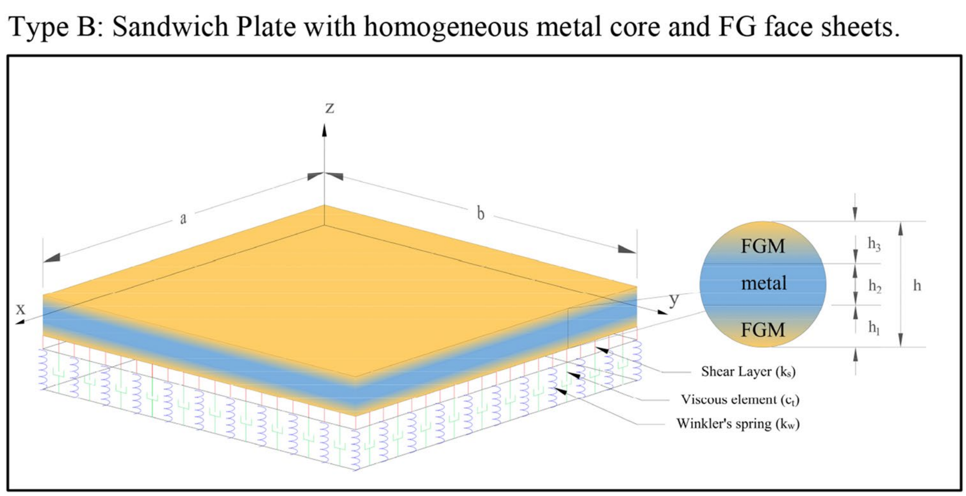

Fig. 2 Illustration of FGSP resting on the viscoelastic foundation: Type B

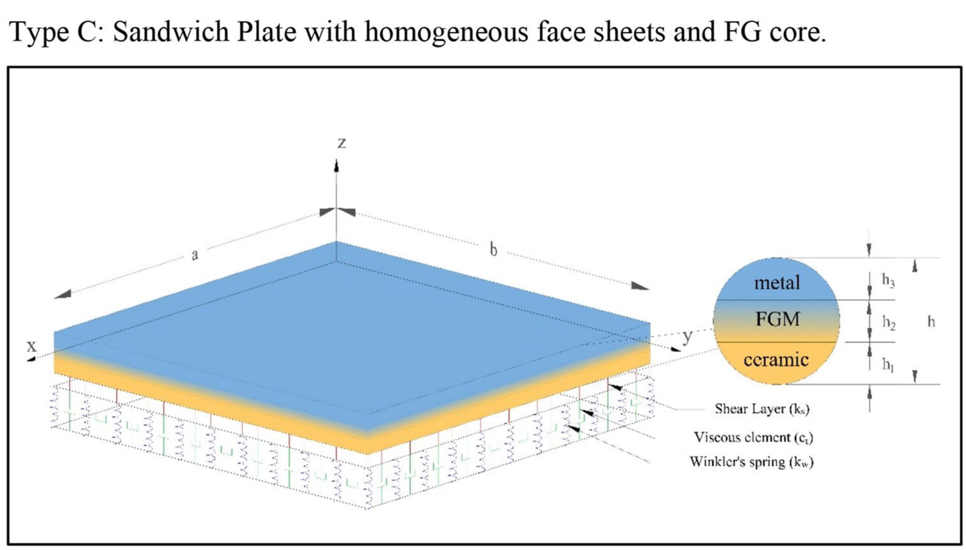

Fig. 3 Illustration of FGSP resting on the viscoelastic foundation: Type C

Table 1 Comparison of non-dimensional natural frequencies $\omega h\sqrt{\rho_c/G_c}$ of a homogeneous square plate without viscoelastic foundations a/h = 10, ν = 0.3

m	n	Exact (Srinivas et al. [43])	Hellal et al. [42]	Present	Sobhy [16]					
					RPT	TPT	SPT	HPT1	EPT	HPT2
1	1	0.09315	0.09304	0.09303	0.09315	0.09303	0.09303	0.09303	0.09304	0.09304
1	2	0.22260	0.22203	0.22198	0.22261	0.22195	0.22198	0.22195	0.22204	0.22200
2	2	0.34207	0.34082	0.34069	0.34215	0.34063	0.34069	0.34063	0.34084	0.34075
1	3	0.41714	0.41535	0.41516	0.41729	0.41507	0.41516	0.41507	0.41538	0.41524
2	3	0.52391	0.52125	0.52096	0.52424	0.52081	0.52096	0.52081	0.52131	0.52109
3	3	0.68893	0.68473	0.68423	0.68974	0.68396	0.68423	0.68395	0.68483	0.68445
2	4	0.75111	0.74628	0.74569	0.75217	0.74536	0.74569	0.74535	0.74640	0.74596
1	5	0.92678	0.92013	0.91922	0.92886	0.91869	0.91922	0.91866	0.92031	0.91963
4	4	1.08890	1.08050	1.07923	1.09232	1.07845	1.07923	1.07842	1.08074	1.07981

Table 2 Comparison of non-dimensional natural frequencies $\omega h\sqrt{\rho_m/E_m}$ of FGM square plate resting on elastic foundation

Method		$\bar{k}_w = 100, \bar{k}_s = 0$				$\bar{k}_w = 100, \bar{k}_s = 100$			
		$h/a = 0.05$	$h/a = 0.1$	$h/a = 0.15$	$h/a = 0.2$	$h/a = 0.05$	$h/a = 0.1$	$h/a = 0.15$	$h/a = 0.2$
Hellal [42]									
	$r = 0$	0.0298	0.1163	0.2520	0.4275	0.0411	0.1619	0.3561	0.6163
	$r = 1$	0.0233	0.0911	0.1983	0.3384	0.0384	0.1520	0.3362	0.5856
	$r = 2$	0.0214	0.0837	0.1819	0.3098	0.0381	0.1505	0.3330	0.5803
	$r = 5$	0.0208	0.0812	0.1760	0.2989	0.0381	0.1507	0.3333	0.5807
Present									
	$r = 0$	0.0298	0.1163	0.2519	0.4274	0.0411	0.1619	0.3561	0.6162
	$r = 1$	0.0233	0.0911	0.1983	0.3383	0.0384	0.1520	0.3361	0.5855
	$r = 2$	0.0214	0.0837	0.1819	0.3098	0.0381	0.1505	0.3330	0.5802
	$r = 5$	0.0205	0.0795	0.1716	0.2900	0.0384	0.1515	0.3349	0.5834

Type B: sandwich plate with homogeneous metal core and FG face sheets.

This type of sandwich plate has a metallic core, whereas the top and bottom layers are FG. The upper surface of the top layer is ceramic, and it is graded to be metallic on its lower face. However, the bottom layer is metallic on the upper face and ceramic on the lower one. The formulation of the volume fraction in this type is defined as follows [42]:

$$\begin{aligned} V_1 &= \left(\frac{2H_1 - 2\bar{z}}{2H_1 + 1}\right)^r, \quad -\frac{1}{2} \le \bar{z} \le H_1, \\ V_2 &= 0, \quad H_1 \le \bar{z} \le H_2, \\ V_3 &= \left(\frac{2H_2 - 2\bar{z}}{2H_2 - 1}\right)^r, \quad H_2 \le \bar{z} \le 1/2. \end{aligned} \tag{3}$$

A plate represents the case of ceramic–metal–ceramic (c–m–c) when $r \to 0$, and its fully homogeneous metallic plate when $r \to \infty$.

Type C: sandwich plate with homogeneous face sheets and FG core.

The top layer is fully ceramic, followed by a core layer, which is functionally graded as ceramic on the upper face and metallic on the lower face. The bottom layer is fully metallic in this type of sandwich plate. The formulation of the volume fraction, in this case, is given by [42]

$$\begin{aligned} V_1 &= 0, \quad \frac{1}{2} \le \bar{z} \le H_1, \\ V_2 &= \left(\frac{\bar{z} - H_1}{H_2 - H_1}\right)^r, \quad H_1 \le \bar{z} \le H_2, \\ V_3 &= 1, \quad H_2 \le \bar{z} \le 1/2. \end{aligned} \tag{4}$$

Table 3 Non-dimensional natural frequencies $\omega h\sqrt{\rho_m/E_m}$ of FGM square plate resting on a viscoelastic foundation

Method	$\overline{k}_w=100,\overline{k}_s=0$				$\overline{k}_w=100,\overline{k}_s=0$			
	$h/a=0.05$	$h/a=0.1$	$h/a=0.15$	$h/a=0.2$	$h/a=0.05$	$h/a=0.1$	$h/a=0.15$	$h/a=0.2$
Present								
$\overline{C}_t=0$								
$r=0$	0.0298	0.1163	0.2519	0.4274	0.0411	0.1619	0.3561	0.6162
$r=1$	0.0233	0.0911	0.1983	0.3383	0.0384	0.1520	0.3361	0.5855
$r=2$	0.0214	0.0837	0.1819	0.3098	0.0381	0.1505	0.3330	0.5802
$r=5$	0.0205	0.0795	0.1716	0.2900	0.0384	0.1515	0.3349	0.5834
$\overline{C}_t=0.05$								
$r=0$	0.0300	0.1169	0.2535	0.4303	0.0412	0.1624	0.3572	0.6182
$r=1$	0.0235	0.0921	0.2006	0.3425	0.0386	0.1526	0.3375	0.5880
$r=2$	0.0217	0.0848	0.1845	0.3147	0.0382	0.1512	0.3345	0.5828
$r=5$	0.0208	0.0808	0.1746	0.2956	0.0385	0.1522	0.3365	0.5862
$\overline{C}_t=0.1$								
$r=0$	0.0301	0.1176	0.2551	0.4332	0.0413	0.1629	0.3583	0.6203
$r=1$	0.0238	0.0931	0.2029	0.3468	0.0387	0.1532	0.3389	0.5905
$r=2$	0.0220	0.0860	0.1872	0.3195	0.0384	0.1518	0.3359	0.5854
$r=5$	0.0211	0.0821	0.1776	0.3011	0.0387	0.1529	0.3380	0.5889
$\overline{C}_t=0.2$								
$r=0$	0.0305	0.1190	0.2582	0.4389	0.0416	0.1639	0.3605	0.6243
$r=1$	0.0243	0.0951	0.2075	0.3550	0.0390	0.1544	0.3416	0.5953
$r=2$	0.0225	0.0883	0.1924	0.3289	0.0387	0.1531	0.3388	0.5906
$r=5$	0.0217	0.0847	0.1834	0.3117	0.0391	0.1543	0.3411	0.5944

2 Problem formulation

2.1 Kinematics and constitutive equations

For the plate in x-, y-, and z-directions, the u, v, and w terms represent the displacement components, respectively. They can be expressed as

$$u(x,y,z,t)=u_0(x,y,t)-z\frac{\mathrm{d}w_0(x,y,t)}{dx}+k_1f(z)\int\theta(x,y,t)\mathrm{d}x, \tag{5}$$

$$v(x,y,z,t)=v_0(x,y,t)-z\frac{\mathrm{d}w_0(x,y,t)}{dy}+k_2f(z)\int\theta(x,y,t)\mathrm{d}y, \tag{6}$$

$$w(x,y,z,t)=w_0(x,y,t), \tag{7}$$

where u_0 and v_0 represent the displacement of the mid-plane of the plate in both directions z and y, respectively. While w_0 and θ are the bending and shear components of transverse displacement (z-direction). k_1 and k_2 are geometry-dependent constants. In this study, a novel shape function $f(z)$ is proposed to satisfy the boundary conditions of zero transverse shear stresses at the top and bottom faces and written as

$$f(z)=\frac{h}{\pi}\sin\left(\frac{\pi z}{h}\right). \tag{8}$$

Considering infinitesimal deformation theory for the plate, the displacements in Eqs. (5)–(7) are evaluated in terms of strains as follows:

$$\epsilon_x=\epsilon_x^0+z\epsilon_x^1+f(z)\epsilon_x^2, \tag{9}$$

$$\epsilon_y=\epsilon_y^0+z\epsilon_y^1+f(z)\epsilon_y^2, \tag{10}$$

$$\epsilon_{xy}=\epsilon_{xy}^0+z\epsilon_{xy}^1+f(z)\epsilon_{xy}^2, \tag{11}$$

$$\gamma_{xz}=g(z)\gamma_{xz,}^0 \tag{12}$$

$$\gamma_{yz} = g(z)\gamma^0_{yz}, \tag{13}$$

where

$$\begin{Bmatrix} \epsilon^0_x \\ \epsilon^1_x \\ \epsilon^2_x \end{Bmatrix} = \begin{Bmatrix} \frac{\partial u_0}{\partial x} \\ -\frac{\partial^2 w_0}{\partial x^2} \\ k_1\theta \end{Bmatrix}, \begin{Bmatrix} \epsilon^0_y \\ \epsilon^1_y \\ \epsilon^2_y \end{Bmatrix} = \begin{Bmatrix} \frac{\partial v_0}{\partial x} \\ -\frac{\partial^2 w_0}{\partial y^2} \\ k_2\theta \end{Bmatrix}, \begin{Bmatrix} \epsilon^0_{xy} \\ \epsilon^1_{xy} \\ \epsilon^2_{xy} \end{Bmatrix} = \begin{Bmatrix} \frac{\partial u_0}{\partial y} + \frac{\partial v_0}{\partial y}x \\ -2\frac{\partial^2 w_0}{\partial x \partial y} \\ k_1 \frac{\partial}{\partial y}\int \theta \, \mathrm{d}x + k_2 \frac{\partial}{\partial x}\int \theta \, \mathrm{d}y \end{Bmatrix},$$

$$\begin{Bmatrix} \gamma^0_{xz} \\ \gamma^0_{yz} \end{Bmatrix} = \begin{Bmatrix} k_1 \int \theta \, \mathrm{d}x \\ k_2 \int \theta \, \mathrm{d}y \end{Bmatrix}, g(z) = \frac{\mathrm{d}f(z)}{\mathrm{d}z}.$$

The shear part, which includes the integrals, has been evaluated using the analogy of the Navier method in which a sinusoidal behavior of transverse displacement is assumed as follows:

$$\frac{\partial}{\partial y}\int \theta \, \mathrm{d}x = A' \frac{\partial^2\theta}{\partial x \partial y}, \ \frac{\partial}{\partial x}\int \theta \, \mathrm{d}y = B' \frac{\partial^2\theta}{\partial x \partial y}, \ \int \theta \, \mathrm{d}x = A' \frac{\partial \theta}{\partial x}, \ \int \theta \, \mathrm{d}y = B' \frac{\partial \theta}{\partial y}, \tag{14}$$

where

$$A' = -\frac{1}{\lambda^2}, \ B' = -\frac{1}{\mu^2}, \ k_1 = \lambda^2, \ k_2 = \mu^2,$$

and

$$\lambda = m\pi/a, \ \mu = \frac{n\pi}{b}.$$

The constitutive relation considered in the formulation of a linear-elastic sandwich plate is as follows:

$$\begin{Bmatrix} \sigma_x \\ \sigma_y \\ \tau_{xy} \\ \tau_{yz} \\ \tau_{xz} \end{Bmatrix}^{(n)} = \begin{bmatrix} C_{11} & C_{12} & 0 & 0 & 0 \\ C_{12} & C_{22} & 0 & 0 & 0 \\ 0 & 0 & C_{66} & 0 & 0 \\ 0 & 0 & 0 & C_{44} & 0 \\ 0 & 0 & 0 & 0 & C_{55} \end{bmatrix}^{(n)} \begin{Bmatrix} \epsilon_x - \alpha\Delta T - \beta\Delta C \\ \epsilon_y - \alpha\Delta T - \beta\Delta C \\ \gamma_{xy} \\ \gamma_{yz} \\ \gamma_{xz} \end{Bmatrix}^{(n)}. \tag{15}$$

Considering $C^{(j)}_{11} = C^{(j)}_{22} = \frac{E^{(j)}(z)}{1-\nu^2}, C^{(j)}_{66} = C^{(j)}_{44} = C^{(j)}_{55} = \frac{E^{(j)}(z)}{2(1+\nu)}$, where ΔT and ΔC represent the temperature and moisture differences, respectively, such as

$$\Delta k = k - k_0, (k = T, C), \tag{16}$$

T_0, C_0 are the reference temperature and moisture, respectively.

2.2 Governing equation

The governing equation used in this paper is developed with the help of Hamilton's Principle, which is stated as follows:

$$\int_0^T (\delta U - \delta K + \delta V) = 0, \tag{17}$$

where δU is the variant of strain energy, δK is the variant of kinetic energy, and δV is the variant of the external work implied by the reaction force of the foundation. The following equation represents the variant of the strain energy of the plate:

$$\begin{aligned} \delta U &= \int_{-h/2}^{h/2} \int_A \left[\sigma_x \delta\epsilon_x + \sigma_y \delta\epsilon_y + \tau_{xy}\delta\gamma_{xy} + \tau_{yz}\delta\gamma_{yz} + \tau_{xz}\delta\gamma_{xz}\right] \mathrm{d}A\mathrm{d}z \\ &= \int_A \Big[N_x \delta\epsilon^0_x + N_y \delta\epsilon^0_y + N_{xy}\delta\gamma^0_{xy} + M^b_x \delta k^b_x \\ &\quad + M^b_y \delta k^b_y + M^b_{xy}\delta k^b_{xy} + M^s_x \delta k^s_x + M^s_y \delta k^s_y + M^s_{xy}\delta k^s_{xy} + S^s_{yz}\delta\gamma_{yz} + S^s_{xz}\delta\gamma_{xz}\Big] \mathrm{d}A. \end{aligned} \tag{18}$$

Considering (A) as the plane surface of the plate in the (x, y) directions, and the terms N, M, and S are defined as

$$\begin{Bmatrix} N_x & N_y & N_{xy} \\ M^b_x & M^b_y & M^b_{xy} \\ M^s_x & M^s_y & M^s_{xy} \end{Bmatrix} = \int_{-h/2}^{h/2} \left(\sigma_x, \sigma_y, \tau_{xy}\right) \begin{Bmatrix} 1 \\ z \\ f(z) \end{Bmatrix} \mathrm{d}z, \tag{19}$$

$$\left(S_{xz}, S_{yz}\right) = \int_{-h/2}^{h/2} \left(g(z)\left(\tau_{xz}, \tau_{yz}\right) \mathrm{d}z.\right.$$

Thereafter, the variation of kinetic energy (δK) is expressed as

$$\delta K = \int_{-h/2}^{h/2} \int_A \rho(z) \left[\frac{\delta u}{\delta t}\delta\left(\frac{\delta u}{\delta t}\right) + \frac{\delta v}{\delta t}\delta\left(\frac{\delta v}{\delta t}\right) + \frac{\delta w}{\delta t}\delta\left(\frac{\delta w}{\delta t}\right)\right] \mathrm{d}A\mathrm{d}z. \tag{20}$$

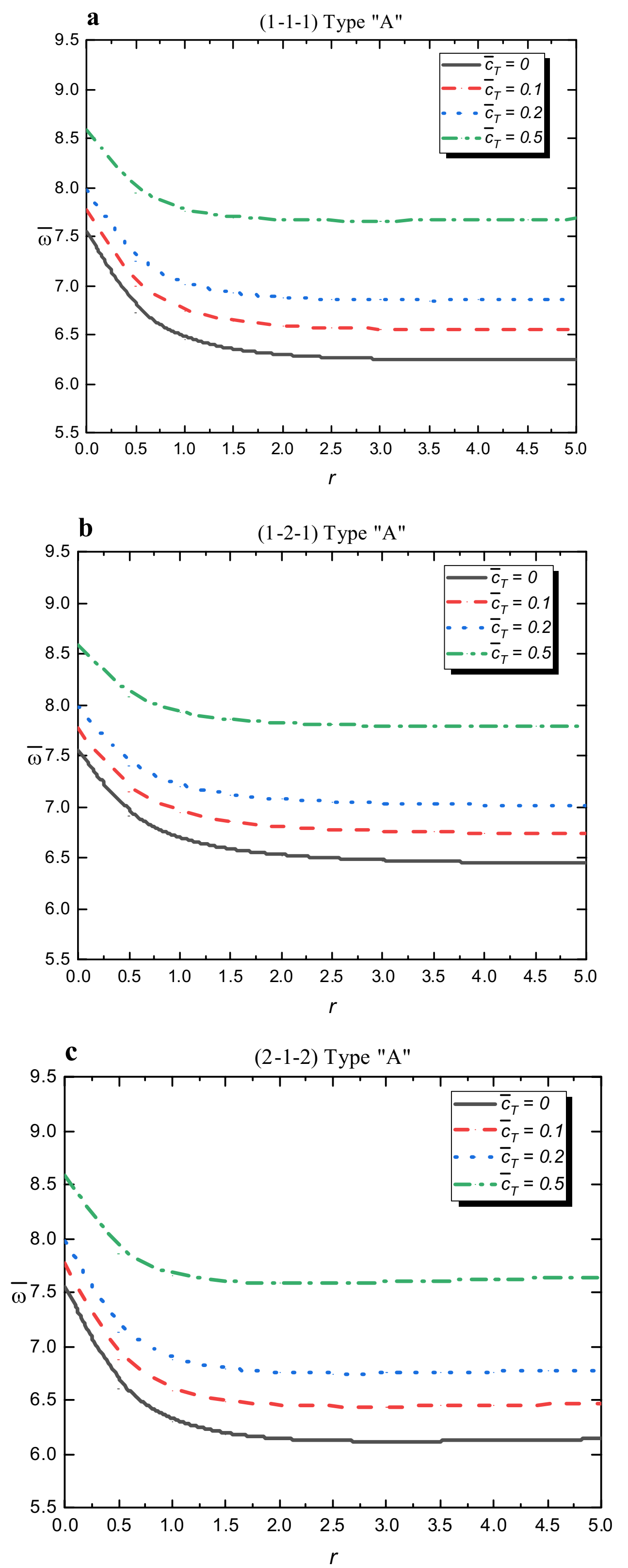

Fig. 4 Effect of the power-law index and damping coefficient on the Eigen frequency $\bar{\omega}$ of FGSP (Type A): ($a/h = 10, b/a = 1, p = 1, \Delta T = 50°\mathrm{C}, \Delta C = 10\,\%, k_w = 100, k_s = 20$) **a**: the (1–1–1) FGSP, **b** the (1–2–1) FGSP, **c** the (2–1–2) FGSP

The variation of external energy caused by the reaction force of the foundation is given by

$$\delta V = \int_A R_f \delta w \mathrm{d}A, \tag{21}$$

where R_f represents the density of the reaction force of the visco-elastic foundation:

$$R_f = \left(k_w - k_s \nabla^2 + c_t \frac{\partial}{\partial t}\right) w(x, y), \tag{22}$$

K_w represents Winkler parameter, while K_s and C_t are the shear layer foundation stiffness and viscosity parameter, respectively.

The governing equation would be a result of solving Eq. (17) using the principle of variational calculus. Thereafter, the solution would be expressed in terms of $\delta u_0, \delta v_0, \delta w_0$ and $\delta\theta$ as

$$\delta u_0 : \frac{\partial N_x}{\partial x} + \frac{\partial N_{xy}}{\partial y} - I_1 \frac{\partial^2 u_0}{\partial t^2} + I_2 \frac{\partial^3 w_0}{\partial x \partial t^2} - I_3 k_1 A' \frac{\partial^3 \theta}{\partial x \partial t^2} = 0, \tag{23}$$

$$\delta v_0 : \frac{\partial N_y}{\partial y} + \frac{\partial N_{xy}}{\partial x} - I_1 \frac{\partial^2 v_0}{\partial t^2} + I_2 \frac{\partial^3 w_0}{\partial y \partial t^2} - I_3 k_2 B' \frac{\partial^3 \theta}{\partial y \partial t^2} = 0, \tag{24}$$

$$\begin{aligned} \delta w_0 : & \frac{\partial^2 M_x^b}{\partial x^2} + \frac{\partial^2 M_y^b}{\partial y^2} + 2\frac{\partial^2 M_{xy}^b}{\partial x \partial y} \\ & - K_w w_0 + K_s \nabla^2 w_0 - c_t \frac{\partial w_0}{\partial t} - I_1 \frac{\partial^2 w_0}{\partial t^2} \\ & - I_2 \left(\frac{\partial^3 u_0}{\partial x \partial t^2} + \frac{\partial^3 v_0}{\partial y \partial t^2} \right) + I_4 \left(\frac{\partial^4 w_0}{\partial x^2 \partial t^2} + \frac{\partial^4 w_0}{\partial y^2 \partial t^2} \right) \\ & - I_5 \left(k_1 A' \frac{\partial^4 \theta}{\partial x^2 \partial t^2} + k_2 B' \frac{\partial^4 \theta}{\partial y^2 \partial t^2} \right) = 0, \end{aligned} \tag{25}$$

$$\begin{aligned} \delta \theta_0 : & - k_1 A' \frac{\partial^2 M_{xs}}{\partial x^2} - k_2 B' \frac{\partial^2 M_{ys}}{\partial y^2} \\ & - \left(k_1 A' + k_2 B'\right) \frac{\partial^2 M_{xy}^s}{\partial x \partial y} + k_1 A' \frac{\partial S_{xz}}{\partial x} \\ & + k_2 B' \frac{\partial S_{yz}}{\partial y} + I_3 \left(k_1 A' \frac{\partial^3 u_0}{\partial x \partial t^2} + k_2 B' \frac{\partial^3 v_0}{\partial y \partial t^2} \right) \\ & - I_5 \left(k_1 A' \frac{\partial^4 w_0}{\partial x^2 \partial t^2} + k_2 B' \frac{\partial^4 w_0}{\partial y^2 \partial t^2} \right) \\ & + I_6 \left(k_1^2 A'^2 \frac{\partial^4 \theta}{\partial x^2 \partial t^2} + k_2^2 B'^2 \frac{\partial^4 \theta}{\partial y^2 \partial t^2} \right) = 0, \end{aligned} \tag{26}$$

where $\left(I_1, I_2, I_3, I_4, I_5, I_6\right)$ are mass inertias, and written as

$$\left(I_1, I_2, I_3, I_4, I_5, I_6\right) = \int_{-h/2}^{h/2} \rho(z) \left(1, z, f, z^2, zf, f^2\right) \mathrm{d}z. \tag{27}$$

Fig. 5 Effect of the power-law index and damping coefficient on the eigenfrequency $\overline{\omega}$ of FGSP (Type B): $(k_w = 100, k_s = 20)$, $(a/h = 10,$ $b/a = 1, p = 1, \Delta T = 50°\text{C}, \Delta C = 10\ \%)$, **a** the (1–1–1) FGSP, **b** the (1–2–1) FGSP, **c** the (2–1–2) FGSP

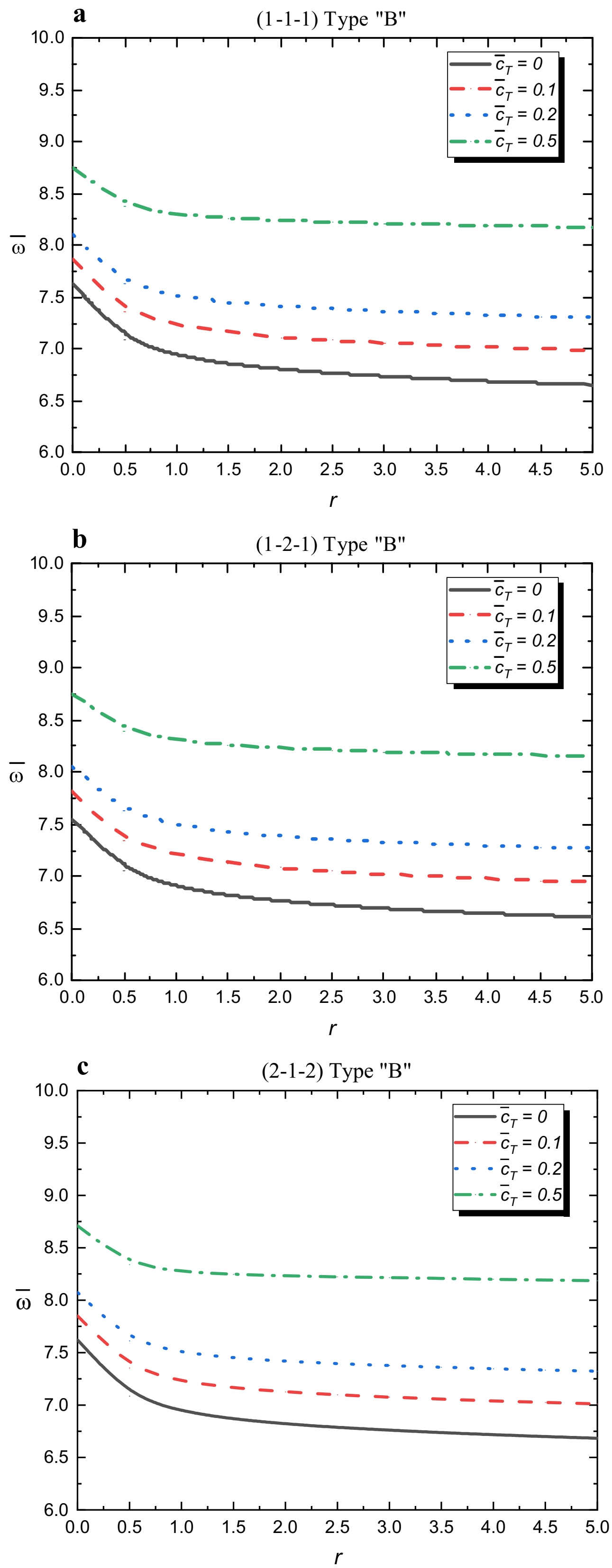

Using the constitutive equation in Eq. (15) and incorporate Eq. (19), the resultant forces of the FG plate including the effect of both temperature and moisture would be evaluated as follows:

$$\begin{Bmatrix} N \\ M^b \\ M^s \end{Bmatrix} = \begin{bmatrix} [A] & [B] & [B^s] \\ [B] & [D] & [D^s] \\ [B^s] & [D^s] & [H^s] \end{bmatrix} \begin{Bmatrix} \epsilon^0 \\ \epsilon^1 \\ \epsilon^2 \end{Bmatrix} + \begin{Bmatrix} N^T \\ M^{bT} \\ M^{sT} \end{Bmatrix} + \begin{Bmatrix} N^C \\ M^{bC} \\ M^{sC} \end{Bmatrix}, \tag{28}$$

$$\begin{Bmatrix} S_{xz} \\ S_{yz} \end{Bmatrix} = \begin{bmatrix} A^s_{44} & 0 \\ 0 & A^s_{55} \end{bmatrix} \begin{Bmatrix} \gamma^0_{xz} \\ \gamma^0_{yz} \end{Bmatrix},$$

where

$$\begin{bmatrix} [A] & [B] & [B^s] \\ [B] & [D] & [D^s] \\ [B^s] & [D^s] & [H^s] \end{bmatrix} = \begin{bmatrix} A_{11} & A_{12} & 0 & B_{11} & B_{12} & 0 & B^s_{11} & B^s_{12} & 0 \\ A_{12} & A_{22} & 0 & B_{12} & B_{22} & 0 & B^s_{12} & B^s_{22} & 0 \\ 0 & 0 & A_{66} & 0 & 0 & B_{66} & 0 & 0 & B^s_{66} \\ B_{11} & B_{12} & 0 & D_{11} & D_{12} & 0 & D^s_{11} & D^s_{12} & 0 \\ B_{12} & B_{22} & 0 & D_{12} & D_{22} & 0 & D^s_{12} & D^s_{22} & 0 \\ 0 & 0 & B_{66} & 0 & 0 & D_{66} & 0 & 0 & D^s_{66} \\ B^s_{11} & B^s_{12} & 0 & D^s_{11} & D^s_{12} & 0 & H^s_{11} & H^s_{12} & 0 \\ B^s_{12} & B^s_{22} & 0 & D^s_{12} & D^s_{22} & 0 & H^s_{12} & H^s_{22} & 0 \\ 0 & 0 & B^s_{66} & 0 & 0 & D^s_{66} & 0 & 0 & H^s_{66} \end{bmatrix},$$

$$\epsilon^0 = \begin{Bmatrix} \epsilon^0_x \\ \epsilon^0_y \\ \epsilon^0_{xy} \end{Bmatrix}, \epsilon^1 = \begin{Bmatrix} \epsilon^1_x \\ \epsilon^1_y \\ \epsilon^1_{xy} \end{Bmatrix}, \epsilon^1 = \begin{Bmatrix} \epsilon^2_x \\ \epsilon^2_y \\ \epsilon^2_{xy} \end{Bmatrix},$$

$$N = \begin{Bmatrix} N_{11} \\ N_{22} \\ N_{12} \end{Bmatrix}, M_b = \begin{Bmatrix} M^b_{11} \\ M^b_{22} \\ M^b_{12} \end{Bmatrix}, M^s = \begin{Bmatrix} M^s_{11} \\ M^s_{22} \\ M^s_{12} \end{Bmatrix},$$

$$N^k = \begin{Bmatrix} N^k_{11} \\ N^k_{22} \\ 0 \end{Bmatrix}, M^{bk} = \begin{Bmatrix} M^{bk}_{11} \\ N^{bk}_{22} \\ 0 \end{Bmatrix}, M^{sk} = \begin{Bmatrix} M^{sk}_{11} \\ M^{sk}_{22} \\ 0 \end{Bmatrix}, \quad k = \{T, C\}.$$

Stiffness elements are evaluated as

$$\left(A_{ij}, A^s_{ij}, B_{ij}, B^s_{ij}, D_{ij}, D^s_{ij}, H^s_{ij}\right) = \int_{(-h/2)}^{(h/2)} \left(1, g(z)^2, z, f(z), z^2, zf(z), f(z)^2 C_{ij} \mathrm{d}z\right), \ (i,j = 1,2 \text{ and } 6)$$

Fig. 6 Effect of the power-law index and damping coefficient on the eigenfrequency $\overline{\omega}$ of FGSP (Type C): ($k_w = 100, k_s = 20$),); ($a/h = 10, b/a = 1, p = 1, \Delta T = 50°\text{C}, \Delta C = 10\%$), **a** the (1–1–1) FGSP, **b** the (1–2–1) FGSP, **c** the (2–1–2) FGSP

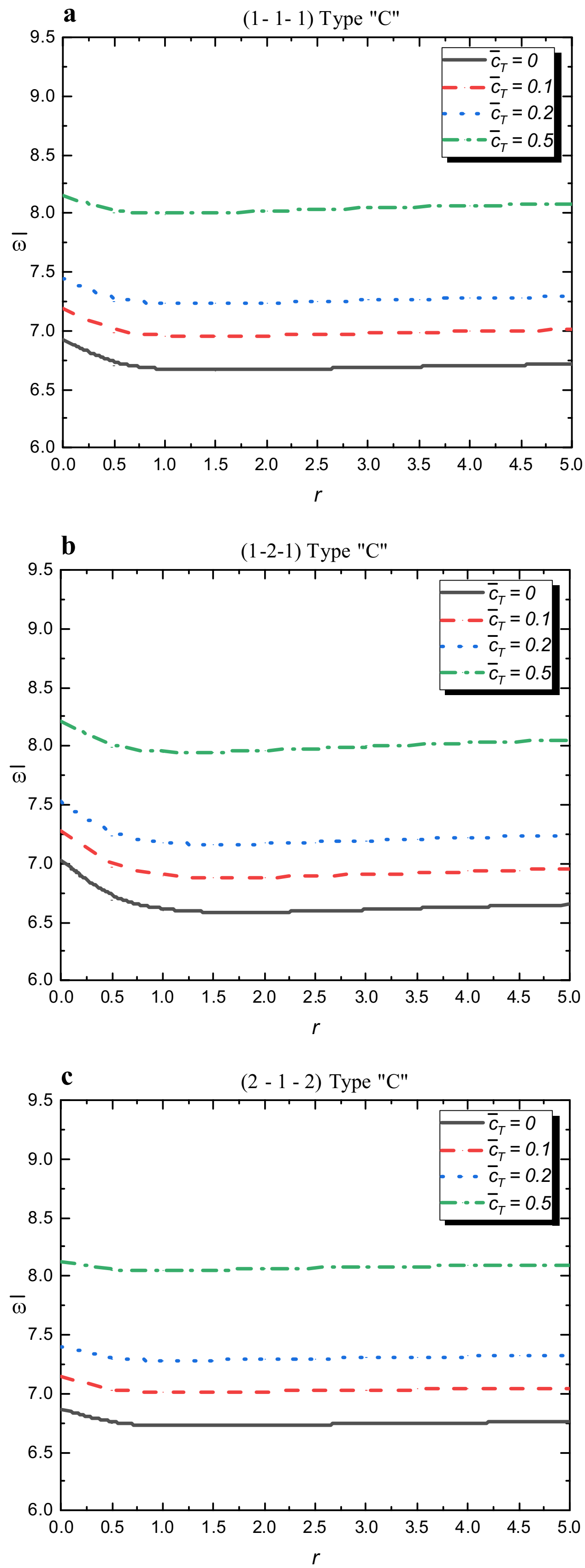

$$A_{ij}^s = \int_{-h/2}^{h/2} C_{ij}\left[g(z)\right]^2 \mathrm{d}z,\ (i,j = 4,5)$$

and

$$\begin{Bmatrix} N_{jj}^T \\ M_{jj}^{bT} \\ M_{jj}^{sT} \end{Bmatrix} = -\sum_{i=1}^{3}\int_{h_i-1}^{h_i}\left(C_{11}+C_{12}\right)T(z)\begin{Bmatrix} 1 \\ z \\ f(z) \end{Bmatrix}\mathrm{d}z, (j = 1,2),$$

$$\begin{Bmatrix} N_{jj}^C \\ M_{jj}^{bC} \\ M_{jj}^{sC} \end{Bmatrix} = -\sum_{i=1}^{3}\int_{h_i-1}^{h_i}\left(C_{11}+C_{12}\right)C(z)\begin{Bmatrix} 1 \\ z \\ f(z) \end{Bmatrix}\mathrm{d}z, (j = 1,2).$$

The applied temperature T and moisture C are assumed to vary along with the thickness of the FGSP, while the variation depends on the exponent P. In the case where $P = 1$, the variation would be linear along with the thickness, while it is nonlinear when $P > 1$ according to the following relation:

$$k(z) = \Delta k\left(\frac{z}{h} + \frac{1}{2}\right)^p + k_b, \quad k = (T, C), \tag{29}$$

where $\Delta T = T_t - T_b$ and $\Delta C = C_t - C_b$ are the temperature and moisture differences, respectively. The subscript t denotes the top surface, while the subscript b is for the bottom surface of the sandwich plate.

3 Analytical solution

The analytical solution for the natural frequency of an FGSP resting on a viscoelastic foundation would be resolved based on a Navier's type solution. The solution only considers the case of simply supported "boundary conditions" by expanding the displacement as a double trigonometric Fourier series as functions of unknown parameters. Therefore, the displacement could be represented as

$$\begin{Bmatrix} u_0 \\ v_0 \\ w_0 \\ \theta \end{Bmatrix} = \sum_{m=1}^{\infty}\sum_{n=1}^{\infty}\begin{Bmatrix} U_{mn}\cos(\lambda x)\sin(\mu y) \\ V_{mn}\sin(\lambda x)\cos(\mu y) \\ W_{mn}\sin(\lambda x)\sin(\mu y) \\ \theta_{mn}\sin(\lambda x)\sin(\mu y) \end{Bmatrix} e^{i\omega_{mn}t}, \tag{30}$$

where U_{mn}, V_{mn}, W_{mn} and θ_{mn} are unknown coefficients, $\lambda = m\pi/a, \mu = n\pi/b$. Also, ω represents the eigenfrequency of the plate at each m and n half wave numbers. The equation of motion would be a result of substituting the Eqs. (30)

Fig. 7 Effect of the temperature difference ΔT on the eigen frequency $\overline{\omega}$ of various types of FGSP; $\left(a/h = 10, r = p = 1, \Delta C = 10\%, k_w = 100, k_s = 20\right)$, **a** Type A, **b** Type B, **c** Type C

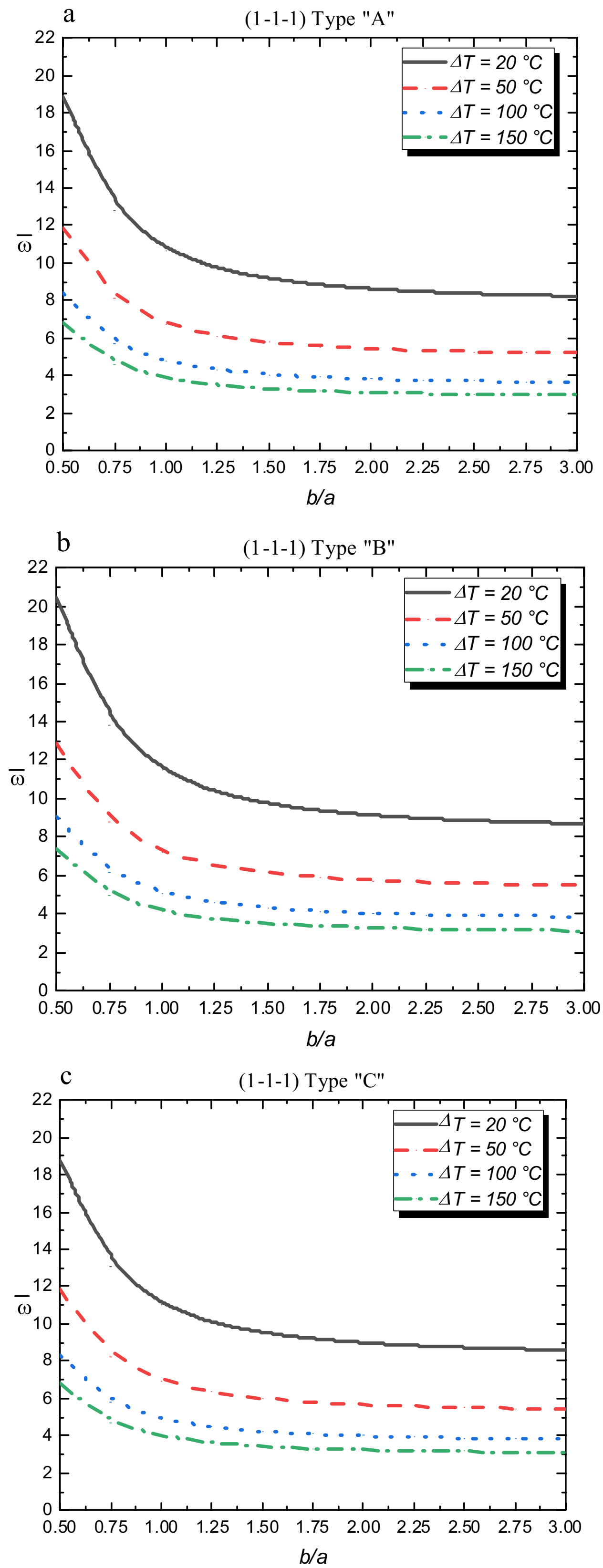

into (23–29). Therefore, it would appear in the form of an Eigen-value problem as

$$\left\{[K] - \omega^2[M]\right\}\{\Delta\} = 0, \tag{31}$$

where

$$\{\Delta\} = \begin{Bmatrix} U_{mn} \\ V_{mn} \\ W_{mn} \\ \theta_{mn} \end{Bmatrix}.$$

Solving Eq. (31) would lead to the following analytical solution:

$$\left(\begin{bmatrix} k_{11} & k_{12} & k_{13} & k_{14} \\ k_{12} & k_{22} & k_{23} & k_{24} \\ k_{13} & k_{23} & k_{33} & k_{34} \\ k_{14} & k_{24} & k_{34} & k_{44} \end{bmatrix} - \omega^2 \begin{bmatrix} m_{11} & m_{12} & m_{13} & m_{14} \\ m_{12} & m_{22} & m_{23} & m_{24} \\ m_{13} & m_{23} & m_{33} & m_{34} \\ m_{14} & m_{24} & m_{34} & m_{44} \end{bmatrix}\right) \begin{Bmatrix} U_{mn} \\ V_{mn} \\ W_{mn} \\ \theta_{mn} \end{Bmatrix} = \begin{Bmatrix} 0 \\ 0 \\ 0 \\ 0 \end{Bmatrix},$$

where

$$k_1 1 = -\lambda^2 A_{11} - \mu^2 A_{66},$$
$$k_{12} = -\lambda\mu\left(A_{12} + A_{66}\right),$$
$$k_{13} = \lambda\mu^2 B_{12} + 2\lambda\mu^2 B_{66} + \lambda^3 B_{11},$$

$$k_{14} = \lambda\mu^2 B^s_{12} + \lambda^3 B^s_{11} + 2\lambda\mu^2 B^s_{66},\ k_{22} = -\mu^2 A_{22} - \lambda^2 A_{66},$$

$$k_{24} = \mu^3 B^s_{22} + \lambda^2\mu B^s_{12} + 2\lambda^2\mu B^s_{66},$$

$$k_{23} = \mu^3 B_{22} + 2\lambda^2\mu B_{66} + \lambda^2\mu B_{12},$$

$$k_{33} = -0.5c_t - K_w - K_s\left(\lambda^2 + \mu^2\right) - 2\lambda^2\mu^2 D_{12} - -\lambda^4 D_{11} - \mu^4 D_{22} - 4\lambda^2\mu^2 D_{66},$$

$$k_{34} = 2\lambda^2\mu^2 D^s_{12} - 4D^s_{66}\lambda^2\mu^2 - \mu^4 D^s_{22} - \lambda^4 D^s_{11},$$

$$k_{44} = -\lambda^2 A^s_{55} - \mu^2 A^s_{44} - 4\lambda^2\mu^2 H^s_{66} - \lambda^4 H^s_{11} - 2\lambda^2\mu^2 H^s_{12} - \mu^4 H^s_{22},$$

$$m_{11} = m_{22} = I_1,\ m_{12} = 0,\ m_{13} = -I_2\lambda,\ m_{14} = -I_3\lambda,$$

Fig. 8 Effect of the temperature difference ΔT and damping ▸ coefficient on the eigenfrequency $\overline{\omega}$ of various types of FGSP; $(a/h = 10, r = p = 1, \Delta C = 10\,\%, k_w = 100, k_s = 20)$: **a** Type A, **b** Type B, **c** Type C

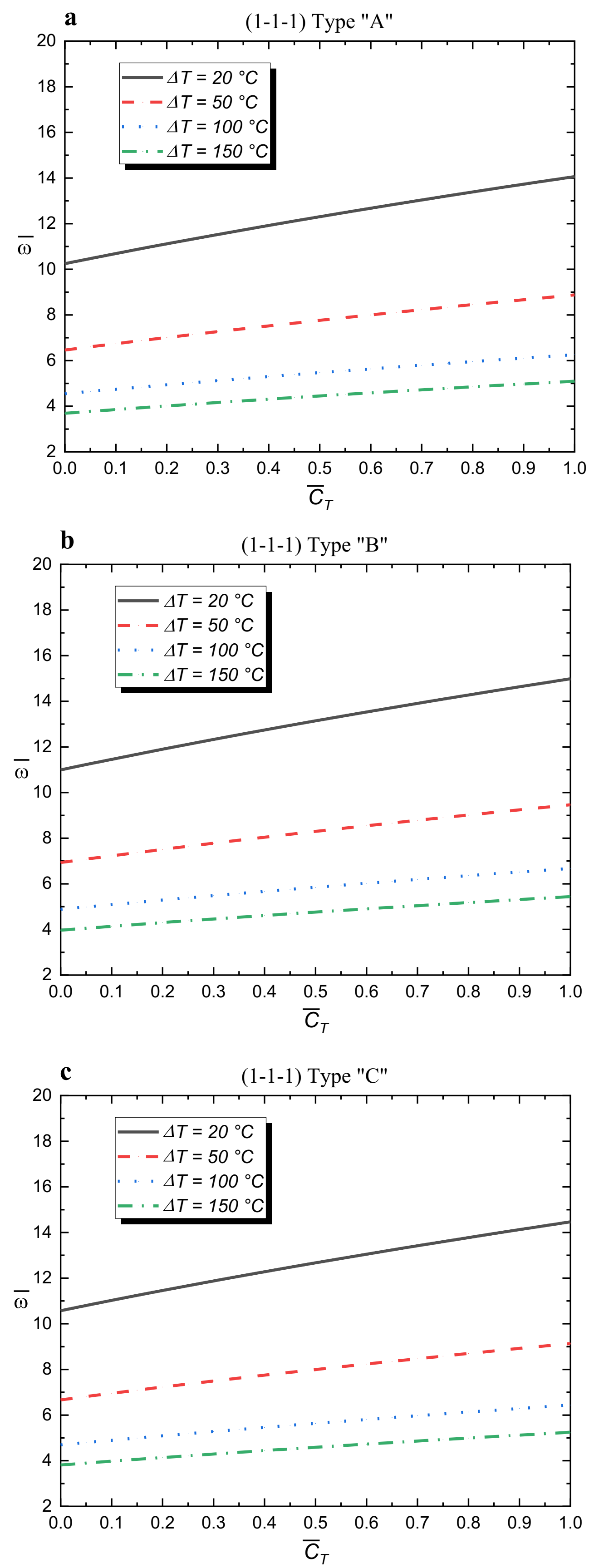

$$
\begin{aligned}
m_{23} &= -I_2 \mu, \\
m_{24} &= -I_3 \mu, \\
m_{33} &= I_1 + \left(\lambda^2 + \mu^2\right) I_4, \\
m_{34} &= \left(\lambda^2 + \mu^2\right) I_5 \\
m_{44} &= \left(\lambda^2 + \mu^2\right) I_6.
\end{aligned}
$$

4 Numerical results

The following parameters have been considered in this study:

$$T_b - T_0 = 25\ ^\circ\mathrm{C}, \quad C_b - C_0 = 0\%$$

and the sandwich plate is composed of metal (aluminum) and ceramic (alumina) material.

- The material properties of Alumina are
  $E_c = 380\,\mathrm{Gpa}, \rho_c = 3800\,\mathrm{kg/m^3}, \alpha_c = 7 \times 10^{-6}(1/^\circ\mathrm{C})$,
  $\beta_c = 0.001\,(\mathrm{wt}\ \%\ \mathrm{H_2O})^{-1}, \nu_c = 0.3$
- The material characteristics of Aluminum are
  $E_m = 70\,\mathrm{Gpa}, \rho_m = 2707\,\mathrm{kg/m^3}, \alpha_m = 23 \times 10^{-6}(1/^\circ\mathrm{C})$,
  $\beta_m = 0.44\,(\mathrm{wt}\ \%\ \mathrm{H_2O})^{-1}, \nu_c = 0.3.$

The solutions in the graphs are shown in non-dimensional units that are proposed as
$\overline{\omega} = \omega h \sqrt{\frac{\rho_c}{G_c \alpha_c \Delta T}}, k_w = \frac{K_w a^4}{D_c}, k_s = \frac{K_s a^2}{D_c}, \quad D_c = \frac{E_c h^3}{12(1-\nu^2)},$
$G_c = \frac{E_c}{2(1+\nu)}, \overline{k}_w = \frac{K_w a^4}{D_m}, \overline{k}_s = \frac{K_s a^2}{D_m}, D_m = \frac{E_m h^3}{12(1-\nu^2)}.$

The novel proposed shear deformation theory is proved in the first place in Table 1 by comparing the natural frequency of a homogeneous square plate excluding a visco-elastic foundation with the exact result published by Sirivas et al. [43]. Furthermore, the proposed theory is also compared with the results obtained by Sobhy [16], in which several theories were used, such as the refined plate theory (RPT), Third-order Plate Theory (TPT), sinusoidal plate theory (SPT), hyperbolic plate theory (HPT1), exponential plate theory (EPT) and HPT2. The comparison concludes that the proposed theory is functioning properly and matches the results of the other previously puplished papers mentioned above. Thereafter, Table 2 includes the effect elastic foundation. The newly proposed theory is compared with Hellal's [42] results for an elastic foundation by considering that the damping coefficient c_t is equal to zero, where the table shows a very good agreement between both theories.

The effect of the damping coefficient (c_t) is tabulated in Table 3, where a non-dimensional natural frequency is calculated for an FGM square plate considering different scenarios of visco-elastic foundation. The effect over the natural frequency is examined among ten different foundation models (two columns representing the elastic part with five rows imitating the viscosity in the foundation). Furthermore, each natural frequency is controlled with respect to the effect of the thickness to length ratio (h/a) and the power-law index; as the value of the damping coefficient increases, the natural frequency increases. The effect would be more significant as the (h/a) and power-index (r) are increasing.

The effect of the damping coefficient of a viscoelastic foundation with respect to the power index r over the natural frequencies is shown in Figs. (4, 5 and 6). Each figure considers one type of FGSP out of the three that were explained earlier with specific geometries. Natural frequency looks to increase as the damping coefficient increases, which would lead to enhancing the rigidity of the plate. The effect of the power index, which varies upon the plate type, is also examined. The natural frequency decreases as the power index increases up to a point where $r = 1$, thereafter the decrement of the natural frequency is minimal. The slope of the first portion of the graph is affected by the ratios between the three layers: as we increase the density of the core (ceramic), the slope tends to decrease. In the case of Type B, the natural frequency behaves similar to Type A. However, the natural frequency in Type B is the maximum among all of the other three types. The plate acquires more rigidity when its core is metal, and the other two faces are FG sheets. Furthermore, the damping coefficient enhances the vibrational response of the plate regardless of the type of the plate.

Figure 7 shows the effect of temperature difference over the natural frequency with respect to the aspect ratio. The results emphasize the fact that the increase in temperature difference reduces the rigidity of the plate significantly. Furthermore, the increase in the aspect ratio reduces the natural frequency. The decrement in the natural frequency for reducing the aspect ratio is less significant when the ratio b/a reaches 1, where the geometry of the plate is square. Whereas an increase in the damping coefficient would enhance the sustainability of the plate linearly in terms of the natural frequency, as in Fig. 8.

The effect of moisture concentration works in a similar way to temperature. The rigidity of the plate is reduced as the moisture concentration increases, as in Fig. 9, where a comparison is carried out using four different moisture concentrations with respect to two different parameters: the aspect ratio and the damping coefficient.

The effect of the temperature study is further extended in Fig. 10 to include the temperature variation. This led to the conclusion that an increase in the temperature variation would elevate the free vibration; a uniform temperature is more severe than the case of linear and nonlinear variation. Finally, the effect of the elastic foundation coefficient (K_w, K_s) along with the damping coefficient c_t is examined in Fig. 11. The natural frequency increases as the coefficient of the viscoelastic foundation increases. The increment is linear along with the damping coefficient.

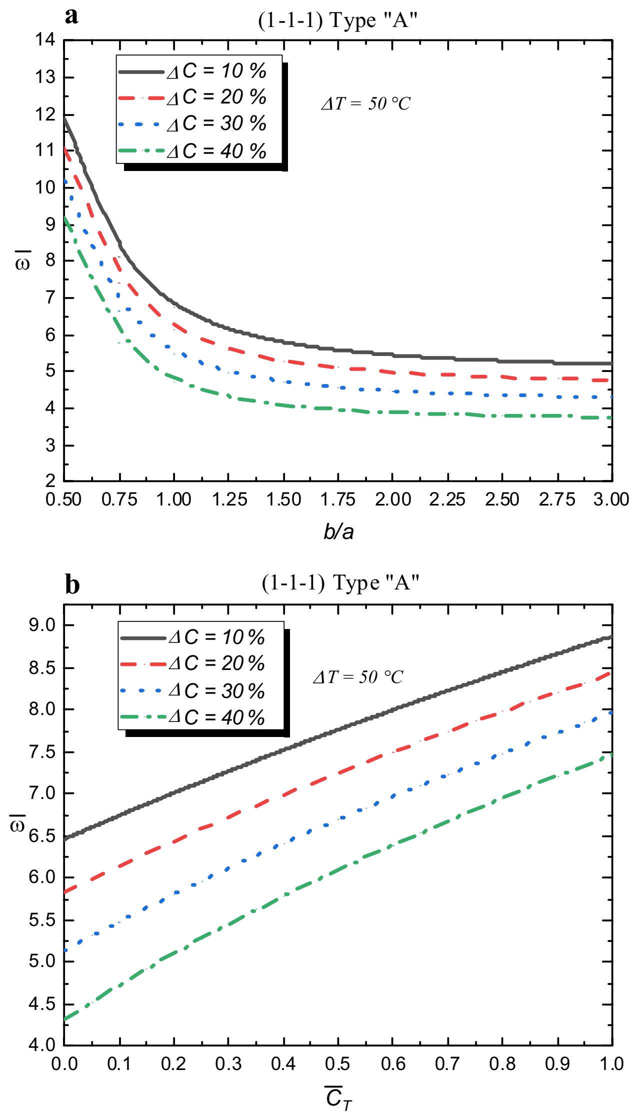

Fig. 9 Effect of the **a** moisture concentration ΔC and **b** damping coefficient on the eigenfrequency $\overline{\omega}$ of FGSP (TypeA) ($a/h = 10, r = p = 1, k_w = 100, k_s = 20$)

5 Conclusions

This work studies for the first time the vibrational behavior of a simply supported FGSP resting on a viscoelastic foundation subjected to a hygro-thermal environment using a newly proposed “four-unknown shear deformation plate theory.” This theory assumes a trigonometric distribution of the shear stress along with the thickness of the plate. Furthermore, a comparison carried out with previously published papers shows a very good agreement. The FGSP is examined considering three different scenarios of the panel’s

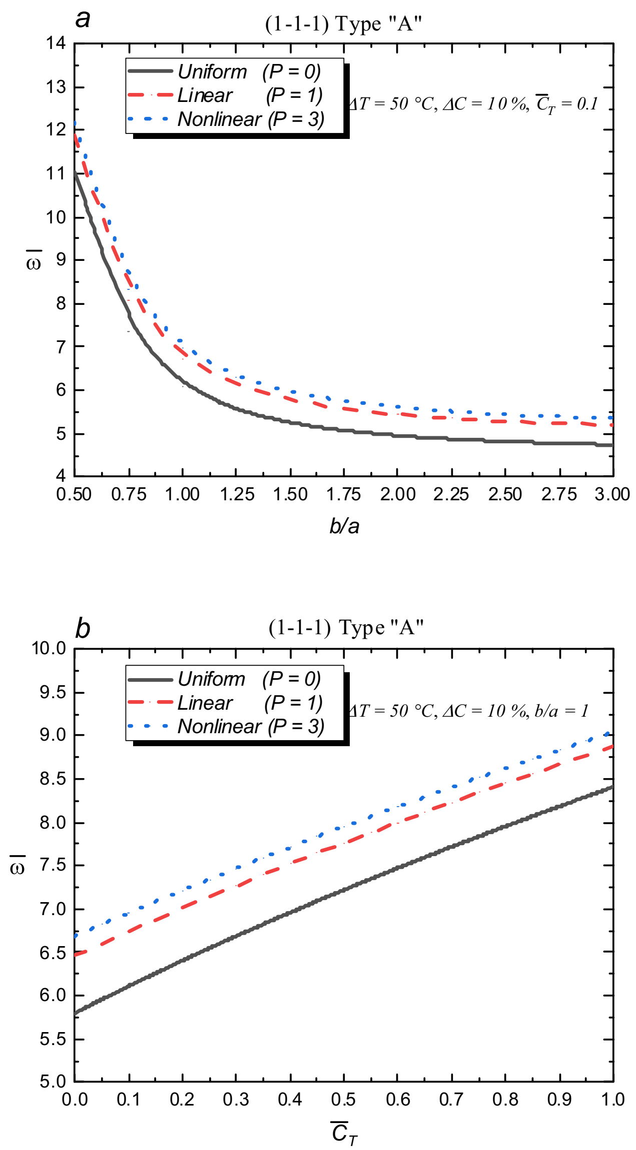

Fig. 10 The variation of the eigenfrequency $\overline{\omega}$ of FGSP (Type A) under various types of hygrothermal with respect to **a** the aspect ratio and **b** the damping coefficient $(a/h = 10, r = p = 1, \Delta T = 50°\mathrm{C}, \Delta C = 10\ \%, k_w = 100, k_s = 20)$

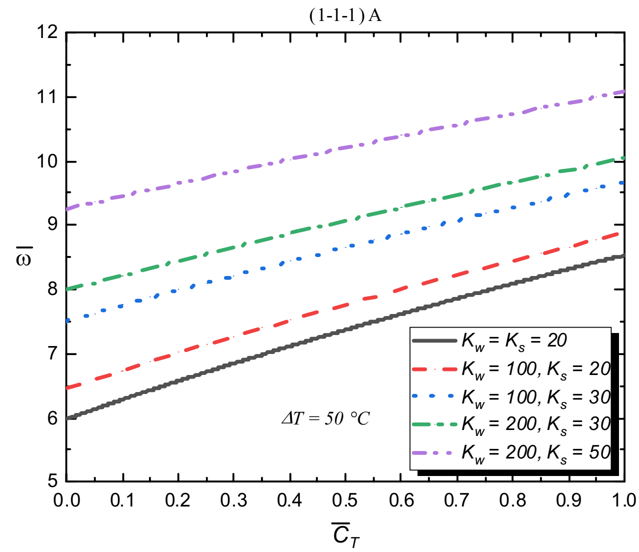

Fig. 11 Effect of the elastic foundation parameters and damping coefficient on the eigenfrequency $\overline{\omega}$ of FGSP of Type A $(a/h = 10, b/a = 1, r = p = 1, \Delta C = 10\%)$

arrangement. This work enhanced the understanding of the impact of the damping coefficient and drew the following conclusions:

- The increase in damping coefficient (c_t) as a property of the viscoelastic foundation would enhance the free-vibrational response of the plate in the same manner among all types of FGSP: Type A, Type B, and Type C.
- The effect of the damping coefficient (c_t) over the natural frequency is not influenced by the plate’s configuration.
- The natural frequency of FGSP is enhanced by the increase in damping coefficient value more significantly when the temperature difference (ΔT) is at low levels.
- At high moisture concentrations, the damping coefficient tends to enhance the rigidity of the plate.
- The change of temperature profile would affect the natural frequency of the plate.

This paper has examined the FGSP in many different aspects considering all of the stated variations, including temperature variation, moisture, aspect ratio, power index, and plate type with different geometries. The analytical solution is obtained with the help of Navier’s solution, whereas Hamilton’s principle is used in the case of the governing equation derivation.

Acknowledgements The authors would like to acknowledge the support provided by the Deanship of Scientific Research (DSR) at King Fahd University of Petroleum and Minerals (KFUPM), Saudi Arabia, for funding this work through Project No. DF181032. The support provided by the Department of Civil and Environmental Engineering is also acknowledged.

References

1. Dai H-L, Rao Y-N, Dai T (2016) A review of recent researches on FGM cylindrical structures under coupled physical interactions, 2000–2015. Compos Struct 152:199–225
2. Dean J, Fallah AS, Brown PM et al (2011) Energy absorption during projectile perforation of lightweight sandwich panels with metallic fibre cores. Compos Struct 93:1089–1095
3. Faleh NM, Ahmed RA, Fenjan RM (2018) On vibrations of porous FG nanoshells. Int J Eng Sci 133:1–14
4. Kolahchi R, Zarei MS, Hajmohammad MH et al (2017) Wave propagation of embedded viscoelastic FG-CNT-reinforced sandwich plates integrated with sensor and actuator based on refined zigzag theory. Int J Mech Sci 130:534–545
5. Mehar K, Panda SK, Mahapatra TR (2018) Nonlinear frequency responses of functionally graded carbon nanotube-reinforced sandwich curved panel under uniform temperature field. Int J Appl Mech 10:1850028
6. Sharma N, Mahapatra TR, Panda SK (2017) Vibro-acoustic analysis of un-baffled curved composite panels with experimental validation. Struct Eng Mech 64:93–107
7. Vinson JR (2005) Sandwich structures: past, present, and future. In: Thomsen OT, Bozhevolnaya E, Lyckegaard A (eds) Sandwich structures 7: advancing with sandwich structures and materials. Springer, Berlin, pp 3–12
8. Zarei MS, Azizkhani MB, Hajmohammad MH et al (2017) Dynamic buckling of polymer–carbon nanotube–fiber multiphase nanocomposite viscoelastic laminated conical shells in hygrothermal environments. J Sandw Struct Mater. https://doi.org/10.1177/1099636217743288
9. Shen H-S. *Functionally Graded Materials: Nonlinear Analysis of Plates and Shells*. 0 ed. CRC Press. Epub ahead of print 19 April 2016. https://doi.org/10.1201/9781420092578.
10. Hajmohammad MH, Azizkhani MB, Kolahchi R (2018) Multiphase nanocomposite viscoelastic laminated conical shells subjected to magneto-hygrothermal loads: dynamic buckling analysis. Int J Mech Sci 137:205–213
11. Kar VR, Panda SK (2016) Nonlinear thermomechanical deformation behaviour of P-FGM shallow spherical shell panel. Chin J Aeronaut 29:173–183
12. Shokravi M (2017) Buckling of sandwich plates with FG-CNT-reinforced layers resting on orthotropic elastic medium using Reddy plate theory. Steel Compos Struct 23:623–631
13. Akavci SS (2016) Mechanical behavior of functionally graded sandwich plates on elastic foundation. Compos Part B Eng 96:136–152
14. Jin G, Su Z, Shi S et al (2014) Three-dimensional exact solution for the free vibration of arbitrarily thick functionally graded rectangular plates with general boundary conditions. Compos Struct 108:565–577
15. Shen H-S, Li S-R (2008) Postbuckling of sandwich plates with FGM face sheets and temperature-dependent properties. Compos Part B Eng 39:332–344
16. Sobhy M (2016) An accurate shear deformation theory for vibration and buckling of FGM sandwich plates in hygrothermal environment. Int J Mech Sci 110:62–77
17. Su Z, Jin G, Wang X et al (2015) Modified fourier-ritz approximation for the free vibration analysis of laminated functionally graded plates with elastic restraints. Int J Appl Mech 07:1550073
18. Wang Z-X, Shen H-S (2013) Nonlinear dynamic response of sandwich plates with FGM face sheets resting on elastic foundations in thermal environments. Ocean Eng 57:99–110
19. Xia X-K, Shen H-S (2008) Vibration of post-buckled sandwich plates with FGM face sheets in a thermal environment. J Sound Vib 314:254–274
20. Yaghoobi H, Yaghoobi P (2013) Buckling analysis of sandwich plates with FGM face sheets resting on elastic foundation with various boundary conditions: an analytical approach. Meccanica 48:2019–2035
21. Ye T, Jin G, Su Z (2014) Three-dimensional vibration analysis of laminated functionally graded spherical shells with general boundary conditions. Compos Struct 116:571–588
22. Rajabi J, Mohammadimehr M (2019) Hydro-thermo-mechanical biaxial buckling analysis of sandwich micro-plate with isotropic/orthotropic cores and piezoelectric/polymeric nanocomposite face sheets based on FSDT on elastic foundations. Steel Compos Struct 33:509–523
23. Zouatnia N, Hadji L (2019) Static and free vibration behavior of functionally graded sandwich plates using a simple higher order shear deformation theory. Adv Mater Res 8:313–335
24. Alibeigloo A, Liew KM (2014) Free vibration analysis of sandwich cylindrical panel with functionally graded core using three-dimensional theory of elasticity. Compos Struct 113:23–30
25. Kirugulige MS, Kitey R, Tippur HV (2005) Dynamic fracture behavior of model sandwich structures with functionally graded core: a feasibility study. Compos Sci Technol 65:1052–1068
26. Sobhani Aragh B, Yas MH (2011) Effect of continuously grading fiber orientation face sheets on vibration of sandwich panels with FGM core. Int J Mech Sci 53:628–638
27. Fu T, Chen Z, Yu H et al (2020) Free vibration of functionally graded sandwich plates based on *n* th-order shear deformation theory via differential quadrature method. J Sandw Struct Mater 22:1660–1680
28. Emdadi M, Mohammadimehr M, Navi BR (2019) Free vibration of an annular sandwich plate with CNTRC facesheets and FG porous cores using Ritz method. Adv Nano Res 7:109–123
29. Nguyen TK, Nguyen TTP, Vo TP, Thai HT (2015) Vibration and buckling analysis of functionally gradedsandwich beams by a new higher-order shear deformation theory. Compos Part B 76:273–285
30. Özütok A, Madenci E (2017) Static analysis of laminated composite beams based on higher-order shear deformation theory by using mixed-type finite element method. Int J Mech Sci 130:234–243
31. Zenkour AM (2005) A comprehensive analysis of functionally graded sandwich plates: part 1—deflection and stresses. Int J Solids Struct 42:5224–5242
32. Meksi R, Benyoucef S, Mahmoudi A et al (2019) An analytical solution for bending, buckling and vibration responses of FGM sandwich plates. J Sandw Struct Mater 21:727–757
33. Di Sciuva M, Sorrenti M (2019) Bending, free vibration and buckling of functionally graded carbon nanotube-reinforced sandwich plates, using the extended refined zigzag theory. Compos Struct 227:111324
34. Mahmoudi A, Benyoucef S, Tounsi A et al (2019) A refined quasi-3D shear deformation theory for thermo-mechanical behavior of functionally graded sandwich plates on elastic foundations. J Sandw Struct Mater 21:1906–1929
35. Ghumare SM, Sayyad AS (2020) Analytical solution using fifth order shear and normal deformation theory for FG plates resting on elastic foundation subjected to hygro-thermo-mechanical loading. Mater Today Proc 21:1089–1093
36. Bellman R, Casti J (1971) Differential quadrature and long-term integration. J Math Anal Appl 34:235–238

37. Madenci E (2021) Free vibration and static analyses of metal-ceramic FG beams via high-order variational MFEM. Steel Compos Struct 39:493–509
38. Madenci E, Gülcü Ş (2020) Optimization of flexure stiffness of FGM beams via artificial neural networks by mixed FEM. Struct Eng Mech 75:633–642
39. Madenci E, Özütok A (2021) Variational approximate for high order bending analysis of laminated composite plates. Struct Eng Mech 73:97–108
40. Madenci E, Özkılıç YO (2021) Cyclic response of self-centering SRC walls with frame beams as boundary. Steel Compos Struct 40:157–173
41. Ebrahimi F, Barati MR (2017) Hygrothermal effects on vibration characteristics of viscoelastic FG nanobeams based on nonlocal strain gradient theory. Compos Struct 159:433–444
42. Hellal H, Bourada M, Hebali H et al (2019) Dynamic and stability analysis of functionally graded material sandwich plates in hygro-thermal environment using a simple higher shear deformation theory. J Sandw Struct Mater. https://doi.org/10.1177/1099636219845841
43. Srinivas S, Joga Rao CV, Rao AK (1970) An exact analysis for vibration of simply-supported homogeneous and laminated thick rectangular plates. J Sound Vib 12:187–199